

# Joint Traffic and Obstacle-aware UAV Positioning Algorithm for Aerial Networks

Kamran Shafafi, André Coelho, Rui Campos, Manuel Ricardo  
INESC TEC and Faculdade de Engenharia, Universidade do Porto, Portugal  
{kamran.shafafi, andre.f.coelho, rui.l.campos, manuel.ricardo}@inesctec.pt

**Abstract**—Unmanned Aerial Vehicles (UAVs) are increasingly used as cost-effective and flexible Wi-Fi Access Points (APs) and cellular Base Stations (BSs) to enhance Quality of Service (QoS). In disaster management scenarios, UAV-based networks provide on-demand wireless connectivity when traditional infrastructures fail. In obstacle-rich environments like urban areas, reliable high-capacity communications links depend on Line-of-Sight (LoS) availability, especially at higher frequencies. Positioning UAVs to consider obstacles and enable LoS communications represents a promising solution that requires further exploration and development.

The main contribution of this paper is the Traffic- and Obstacle-aware UAV Positioning Algorithm (TOPA). TOPA takes into account the users' traffic demand and the need for LoS between the UAV and the ground users in the presence of obstacles. The network performance achieved when using TOPA was evaluated through ns-3 simulations. The results show up to 100% improvement in the aggregate throughput without compromising fairness.

**Index Terms**—Unmanned Aerial Vehicles, Aerial Networks, UAV Placement, Positioning Algorithm, LoS communications, Obstacle Detection.

## I. INTRODUCTION

In recent years, Unmanned Aerial Vehicles (UAVs) gained attention for deploying versatile Wi-Fi Access Points (APs) and cellular Base Stations (BSs) due to low cost and flexible deployment [1], [2]. UAV-based networks offer unique advantages, especially in disaster management scenarios such as wildfires, earthquakes, floods, cyber, and terrorist attacks, where traditional infrastructures may fail [3]. The need to enhance wireless network coverage for ubiquitous Internet access is crucial in today's digital society, enabling various online services and applications such as ultra-high definition videos, online games, augmented reality, disaster safety, and event facilitation.

In this context, Flying Networks (FNs), formed by UAVs, balloons, and airships, have emerged as an effective and flexible solution to provide wireless communications anywhere and anytime [4], [5]. By using the capabilities of UAVs, FNs can outperform traditional terrestrial networks and provide communications in remote areas, disaster-stricken regions, and extreme environments. However, the successful deployment and operation of FNs introduce their own challenges. One of the key challenges is to ensure Line-of-Sight (LoS) availability at high frequencies, in which the radio signal propagation can be easily obstructed by obstacles, such as buildings,

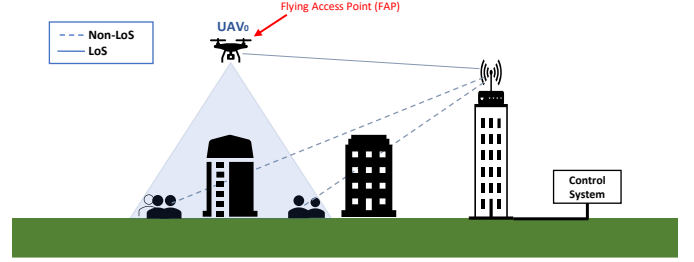


Fig. 1. Flying network consisting of UAV positioned to provide LoS wireless connectivity. The users are served by the UAV, which is connected to the LTE Base Station (BS).

vegetation, and terrain irregularities. These obstructions can significantly limit the coverage range and reliability of FNs.

To overcome this challenge, as depicted in Fig. 1, the solution lies in exploring positioning approaches for UAVs to ensure LoS and optimize network performance. By optimally positioning UAVs, it becomes possible to establish LoS communications links between UAVs and User Equipment (UE), ensuring maximum network performance even in environments with obstacles. However, existing solutions for improving wireless network coverage typically overlook the presence of obstacles in the environment or do not fully address the challenges associated with positioning the FNs in such scenarios [6]–[10].

The main contribution of this paper is the Traffic- and Obstacle-aware UAV Positioning Algorithm (TOPA). TOPA takes into account the users' traffic demand and the need for LoS between the UAV and the ground users in the presence of obstacles. TOPA is designed to address the challenges posed by environments with obstacles, ensuring LoS connectivity and meeting the traffic demand of each user. By integrating traffic awareness into the positioning algorithm, TOPA establishes high throughput communications links with high enough capacity to accommodate the user traffic demand. Simulation results using Network Simulator (ns-3) validate the effectiveness of TOPA in improving network performance and ensuring LoS, particularly in terms of aggregate throughput between the ground users and the UAV.

The rest of this paper is organized as follows. Section II provides an overview of the state-of-the-art positioning approaches in FNs. Section III introduces the system model. Section IV formulates the problem. Section V

presents the TOPA, including its underlying rationale and a demonstration for a simplified scenario. Section VI focuses on the performance evaluation, including the simulation setup, scenarios, performance metrics, and simulation results. Finally, Section VII point out the main conclusions and outlines potential future work directions.

## II. STATE OF THE ART

In this section, we provide a review of the existing solutions in the literature regarding the positioning problem of FNs and highlight their major limitations.

The research works mentioned in this paragraph primarily focus on obstacle-free environments, neglecting the impact of obstacles on LoS. In [6], a traffic-aware positioning solution was proposed to meet user traffic demand. The UAV's position is adjusted based on the estimated user location on the ground. Similarly, [7] presents a heuristic positioning solution for a set of UAVs functioning as a backhaul network. [8] introduces a centralized routing solution for a flying multi-hop network, aiming to establish high-capacity paths between UAVs. In [9], a proactive queue management solution for FNs with controlled topology was proposed, in order to define the UAV queue size over time to maximize throughput while ensuring stochastic delay guarantees. [11] proposes an optimal 3D deployment strategy for multiple UAVs to maximize downlink coverage performance while minimizing transmission power. [12] focuses on utilizing UAVs as flying Base Stations (BSs), optimizing the number of UAVs required to provide coverage for the users. However, these works can be enhanced by considering the presence of obstacles.

There are other state-of-the-art works that specifically address the issue of potential blockages faced by UEs when encountering obstacles. In [13], the authors propose an end-to-end system that tackles the blockage prediction problem for UEs by leveraging point cloud processing and deep learning techniques. Another solution presented in [14] proactively predicts dynamic link blockages between a 5G BS and the user, utilizing video-based approaches. Furthermore, [15] demonstrates how computer vision techniques enable look-ahead prediction in scenarios involving millimeter-wave channel blockages, enabling proactive measures before the actual blockage occurs. However, these works primarily focus on providing wireless paths through terrestrial BSs and overlook the positioning of UAVs in FNs.

## III. SYSTEM MODEL

The system model consists of: i) a UAV as a Flying AP (FAP) to provide wireless communications to the users; ii)  $N-1$  UEs distributed in the venue and waiting to be served by FAP; iii) a building as obstacle deployed in the scenario; iv) a Control System (CS) that can be deployed anywhere in the cloud, edge, or in the UAV, as depicted in Fig. 1. The scenario aims to take advantage of short-range, high-directional air-to-ground radio links. In more crowded scenarios, an effective approach is to increase the number of UAVs and create isolated scenarios, with each UAV assigned to a specific set of

UEs. This allows for better resource allocation and improved network efficiency. In this paper, we focus on the single-UAV scenario and leave the multi-UAV scenarios for future work.

The CS is responsible for: 1) collecting the coordinates of the UEs on the ground by running a Position Recognition Algorithm (PRA) such as the one presented in [16] or similar algorithms to determine the coordinates of the UEs – this information is critical for positioning the UAV; 2) updating the coordinates of the obstacles using the map of the venue – Herein, only buildings are considered as obstacles, leaving the consideration of moving obstacles, like cars, for future research; 3) determining the updated position of the UAV, taking into account the provided information, to establish LoS with all UEs and accommodate their traffic demand. The resulting optimal positions are sent by the CS to the UAV, which positions itself accordingly.

## IV. PROBLEM FORMULATION

The flying network is represented by a directed graph,  $G(t_k) = (U, L(t_k))$ , where  $t_k = k \times \Delta t, k \in \mathbb{N}_0$  and  $\Delta t \in \mathbb{R}$ , represents the time instant to update the UEs position by PRA.  $U$  comprises  $N$  nodes forming the network, including all the UEs and the UAV. The links between the UEs and the UAV at time  $t_k$  are represented by the set  $L(t_k)$ .

Let us consider the  $UE_i$ , where  $i \in \{1, \dots, N-1\}$ , transmits a traffic flow of bitrate  $T_i(t_k)$  bit/s during time slot  $t_k$  to the UAV. The flow bitrate,  $T_i(t_k)$ , in bit/s requires a minimum capacity  $C_i(t_k)$ , in bit/s, for the bidirectional wireless link between  $UE_i$  and the UAV at time  $t_k$ . The flow is received at the UAV from  $UE_i$  with a bitrate of  $R_i(t_k)$  bit/s. The maximum channel capacity is  $C^{MAX}$  bit/s. We assume the wireless medium is shared, the UAV has the ability to listen to any  $UE_i$ , and the Carrier Sense Multiple Access with Collision Avoidance (CSMA/CA) mechanism is employed for Medium Access Control (MAC).

Our objective is to determine, at any given time  $t_k$ , the position of the UAV, represented as  $P = (x, y, z)$ , which ensures LoS connectivity with all UEs. Additionally, we aim to determine the transmission power  $P_T$  of the UEs which we assume will be equal for all of them. This computation takes into account the following rationale: the maximum transmission power  $P_T^{MAX}$  allowed for the wireless technology used ensures that the capacity  $C_i(t_k)$  is sufficient to accommodate the bitrate  $T_i(t_k)$  while minimizing the  $C(t_k) = \sum_{i=1}^{N-1} C_i(t_k)$ , where  $C(t_k)$  is the overall network capacity. By minimizing the  $C(t_k)$ , we can reduce the required transmission power, leading to less interference between nodes and lower energy consumption. In our scenario,  $\theta_{i1}$  is the angle between the ground and the line that passes through  $UE_i$  and the corner of the building closest to  $UE_i$  (solid lines in Fig. 2) and  $\theta_{i2}$  is the angle between the ground and the line that passes through  $UE_i$  and the UAV (dashed line in Fig. 2).

In simple terms, the problem can be formulated as defined in (1a).

$$\begin{aligned}
& \underset{P_T, (x, y, z)}{\text{minimize}} \quad C(t_k) = \sum_{i=1}^{N-1} C_i(t_k) & (1a) \\
& \text{subject to: } 0 \leq P_T \leq P_T^{MAX} & (1b) \\
& \quad C(t_k) \leq C^{MAX} & (1c) \\
& \quad 0 < T_i(t_k) \leq C_i(t_k) \quad i \in \{1, \dots, N-1\} & (1d) \\
& \quad 0 \leq (x, y, z) \leq (x^{MAX}, y^{MAX}, z^{MAX}) & (1e) \\
& \quad \theta_{i1} \leq \theta_{i2}, \quad i \in \{1, \dots, N-1\} & (1f)
\end{aligned}$$

Where,  $(x^{MAX}, y^{MAX}, z^{MAX})$  is the maximum coordinate allowed, in which the UAV can be deployed to accommodate the  $T_i(t_k)$ .

## V. TRAFFIC- AND OBSTACLE-AWARE POSITIONING ALGORITHM

The target positioning subspace ( $P_s$ ) is identified as the area for positioning the UAV, as depicted in Fig. 2. All the points in this subspace are in LoS with all UEs and satisfy their traffic demands. Among these points,  $P = (x, y, z)$ , the optimal position, minimizes both the sumrates and the transmitted energy.

First, TOPA assumes the environment is free of obstacles. This stage aims at ensuring that the wireless link established between  $UE_i$  and the UAV has a minimum Signal-to-Noise Ratio (SNR), denoted as  $SNR_i$ , which enables the utilization of an appropriate Modulation and Coding Scheme (MCS) index, denoted as  $MCS_i$ . The selected  $MCS_i$  should be capable of transporting  $T_i$  bit/s. By guaranteeing the conditions for  $MCS_i$ , we can ensure that the network has the capacity to accommodate  $T_i$ , thereby maximizing the amount of data received at the UAV,  $R(t_k)$ . Additionally, the selection of  $MCS_i$  imposes a minimum  $SNR_i$ , assuming a constant noise power  $P_N$ . Given the known transmission power  $P_T$ , we can calculate the maximum distance  $d_{max_i}$  between  $UE_i$  and the UAV using the Free-space path loss model defined in Eq. 2 in dB, where  $f_i$  represents the carrier frequency, in Hz, and  $c$  corresponds to the speed of light in vacuum.

$$SNR_i = P_T - 20 \log_{10}(d_{max_i}) - 20 \log_{10}(f_i) - 20 \log_{10}\left(\frac{4 \times \pi}{c}\right) - P_N \quad (2)$$

Taking into account  $N - 1$  UEs, the target positioning subspace  $P_s$  for placing the UAV is determined by the intersection of the spheres centered at each  $UE_i$ . The maximum distance  $d_{max_i}$  represents the radius of the sphere centered at  $UE_i$ , indicating the range within which the UAV should be positioned. By solving Eq. (3), derived from Eq. (2) for each  $UE_i$  at  $(x_i, y_i, z_i)$ , TOPA calculates the UAV coordinates,  $(x, y, z)$ .

$$\begin{aligned}
(x - x_i)^2 + (y - y_i)^2 + (z - z_i)^2 &\leq \left(10^{\frac{K + P_T - SNR_i}{20}}\right)^2 \\
K &= -20 \log_{10}(f_i) - 20 \log_{10}\left(\frac{4 \times \pi}{c}\right) - (P_N)
\end{aligned} \quad (3)$$

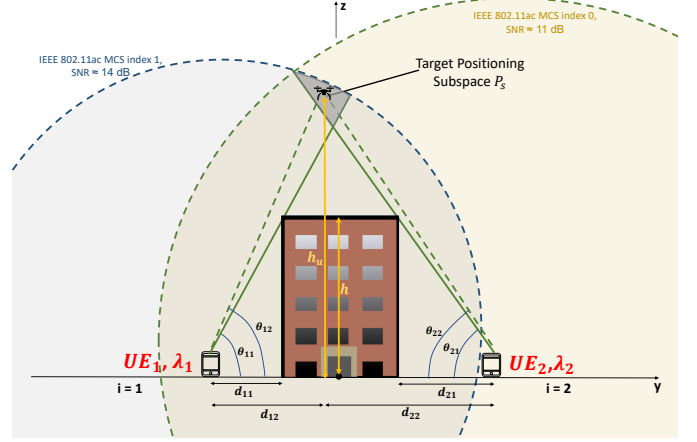


Fig. 2. Two-dimensional (2D) representation of the target positioning subspace ( $P_s$ ), which is determined by the intersection of LoS constraints derived from the obstacle and the traffic demand spheres centered at each UE.

Secondly, TOPA focuses on enforcing constraints to ensure LoS connectivity between the UEs and the UAV, resulting in the positioning subspace  $P_s$ . As depicted in Fig. 2, for establishment LoS,  $\theta_{i1} = \arctan\left(\frac{d_{i1}}{h}\right) \leq \theta_{i2} = \arctan\left(\frac{d_{i2}}{h_u}\right)$ .

$P_s$  is obtained by considering the volume defined by the intersection of the spheres centered at each  $UE_i$  and the lines defining the angle  $\theta_{i2}$  with the ground.  $P_s$  is represented by the gray area in Fig. 2. TOPA assumes symmetry links and constant transmission power for all UEs and the UAV.

### Algorithm A – TOPA

```

1:  $P_T = 0$  ▷ 0 dBm TX power
2: while  $P_T \leq P_T^{MAX}$  do ▷ Allowed TX power
3:    $P_{T_i} = P_T, i \in \{1, \dots, N-1\}$  ▷ UEs' TX power
4:   if  $(x, y, z) \leq (x^{MAX}, y^{MAX}, z^{MAX})$  then
5:     if  $\theta_{i1} \leq \theta_{i2}$  then
6:       Calculate  $(x_0, y_0, z_0)$ 
7:       if  $(x, y, z) \neq \emptyset$  then ▷  $(x, y, z) \in P_s$ 
8:         return  $P_T, (x, y, z)$ 
9:       else
10:         $P_T = P_T + 1$  ▷ Increase TX power by 1 dBm
11:      end if
12:    end if
13:  end if
14: end while

```

We provide an illustrative example of the execution of TOPA in the scenario depicted in Fig. 2. TOPA can be used in scenarios consisting of  $N - 1$  UEs, one UAV, and one obstacle. For illustration purposes, we assume the obstacle has dimensions of (10, 10, 20) meters, respectively length, width, and height. We also consider two UEs,  $UE_1$  and  $UE_2$ , which are located at coordinates (0, -15, 1) and (0, 20, 1), respectively; we consider an altitude of 1 m for each UE to represent UEs carried by people. We consider the utilization of the IEEE 802.11ac standard with one spatial stream, a Guard Interval (GI) of 800 ns, and channel bandwidth of 160 MHz (channel 50 at 5250 MHz). We assume that the demanded capacity for  $UE_1$  is 117 Mbit/s, associated with

the IEEE 802.11ac MCS index 1, and the demanded capacity for  $UE_2$  is 58.5 Mbit/s, associated with the IEEE 802.11ac MCS index 0 [17]. These target MCS indexes are considered to illustrate the execution of Algorithm A where  $UE_1$  has a traffic demand two times higher than  $UE_2$ .

Based on the minimum Received Signal Strength Indicator (RSSI) values proposed in [17] and a noise floor power of  $-85$  dBm, the minimum target SNR values in dB are 14 dB for  $UE_1$  and 11 dB for  $UE_2$ . By solving the system of equations (3) derived from the Friis propagation model (2), consideration the LoS constraint by (1f), and replacing  $k$  from (4), we determine the optimal position for the UAV and its transmission power using the optimization solver *GEKKO*. The optimal position is  $(x, y, z) \approx (0.0, -1.48, 29.44)$ , with a transmission power  $P_T$  of 6 dBm. The parameter  $P_T$  in (3) serves as a fine-tuning parameter and is initially set to 0 dBm. The algorithm proceeds by incrementing the value of  $P_T$  in steps of 1 dBm until a valid solution is achieved. If no solution is found within the specified range, the execution of TOPA is halted. TOPA aims at reducing the distances of wireless links while ensuring that the transmission power  $P_T$  remains within the prescribed maximum value  $P_T^{\text{MAX}}$ .

$$K = -20 \log_{10}(5250 \times 10^6) - 20 \log_{10}\left(\frac{4 \times \pi}{3 \times 10^8}\right) - (-85) \quad (4)$$

## VI. PERFORMANCE EVALUATION

This section presents the simulation setup, an overview of the simulation scenarios used, and an analysis of the simulation results obtained for TOPA using ns-3.

### A. Simulation Setup

We developed a framework in ns-3 to evaluate the performance of the proposed algorithm. In this framework, we deployed the building as a static obstacle using *BuildingModel* and the users in a fixed position with *ConstantPositionMobilityModel*. A Network Interface Card (NIC) was configured on UAV in Ad Hoc mode, using the IEEE 802.11ac standard in channel 50, with a channel bandwidth of 160 MHz, and GI of 800 ns. One spatial stream was used for all links between UEs and the UAV. UDP traffic was generated by the *OnOffApplicationModule* on each UE, while a UDP sink receiver was installed on the UAV. The framework evaluates the scenarios in two phases.

In the first phase, based on the coordinates of the UEs and the position of the UAV, the framework checks the channel condition regarding the establishment of LoS or NLoS links between the UAV and the UEs considering the obstacles. The *ItuR1411LosPropagationLossModel* is applied when the UAV has LoS with UEs. Otherwise, the *ItuR1411NlosOverRooftopPropagationLossModel* is applied.

In the second phase, the performance of the network is evaluated by generating UDP traffic with a constant packet size of 1024 bytes. The data rate is adjusted to meet each UEs' traffic demand, ensuring compatibility and efficient data transmission. The *IdealWifiManager* auto rate mechanism

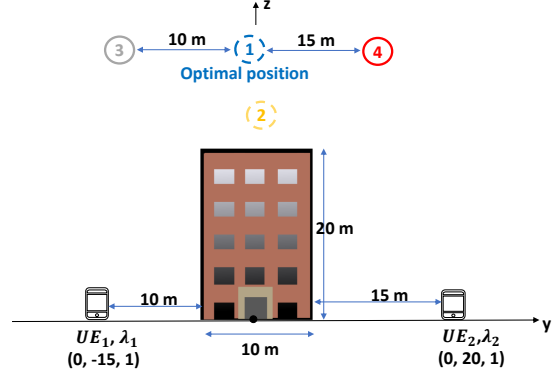


Fig. 3. Scenario A – two UEs and four possible positions. Position 1 is the optimal solution defined by TOPA, which allows LoS with all UEs, while Position 2 is the baseline, which is located five meters above the middle of the rooftop of the building.

was utilized. The simulation is conducted over a duration of 100 seconds, measuring the aggregate throughput on the UAV. The evaluation interval is set to 1s to capture the average aggregate throughput over time.

### B. Simulation Scenarios

We have considered two scenarios to evaluate the performance of TOPA. For scenario A, depicted in Fig. 3, the optimal position achieved by TOPA (Position 1) provides LoS connectivity with both UEs over the rooftop. In order to assess the performance of TOPA, we consider a total of 4 positions, including the point, which is randomly located above the middle of the rooftop of the building (Position 2). Position 3 and position 4 are located, respectively, in LoS with  $UE_1$  and  $UE_2$ . To make the evaluation of TOPA more realistic and suitable for heterogeneous scenarios, we introduce varying traffic demands for the UEs. Specifically, the traffic demand of  $UE_1$  is set to be twice the traffic demand of  $UE_2$ . This difference in traffic demands allows us to assess the performance of TOPA under varying load conditions and capture the impact of asymmetrical traffic requirements ( $\lambda_1 = 2 \times \lambda_2$ ).

Scenario B, depicted in Fig. 4, aims at demonstrating the versatility and effectiveness of TOPA in crowded scenarios with multiple UEs. This scenario serves as a reference to assess the performance and capabilities of TOPA in challenging and densely populated environments. To simulate a diverse and realistic environment, we have divided the UEs into four groups located on different sides of the building; without loss of generality, the groups are placed in front of each facade of the building. Each group is represented by a square with dimensions of  $1m \times 1m$ , and the center of each square corresponds to the location of the respective group. This simplification allows us to capture the spatial distribution of UEs in the scenario while maintaining a manageable representation of their positions. Each group has its own traffic demand, which is presented by  $\lambda_i, i \in \{1, \dots, N-1\}$ . The scenario is evaluated in a total of 6 positions to assess the performance of TOPA. Position 1 represents the optimal placement achieved by TOPA, which maximizes

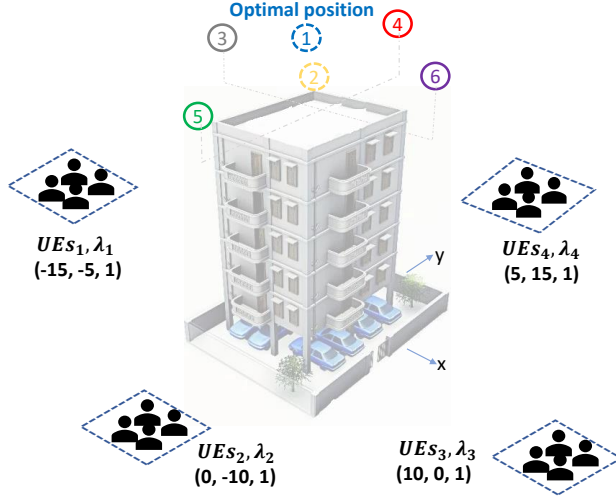


Fig. 4. Scenario B – four groups of UEs located on different sides of the building. Each group is represented by a square with dimensions of  $1m \times 1m$  and associated traffic demand that is presented by  $\lambda_i, i \in \{1, \dots, N-1\}$ .

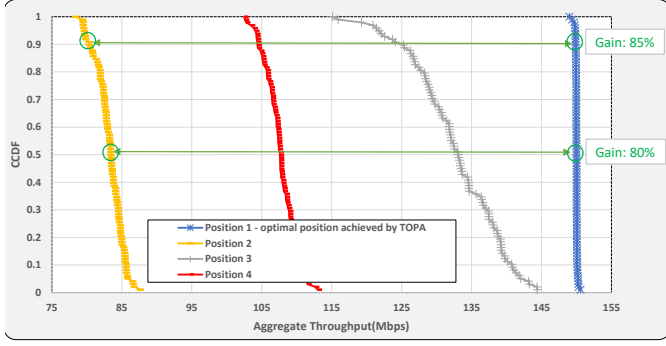


Fig. 5. Scenario A - Aggregate throughput measured on UAV, where  $\lambda_1 = 2 \times \lambda_2$ .

network throughput. The remaining positions are situated on different sides of the building and (Position 2) is randomly located above the middle of the rooftop of the building. Based on the same rationale, three different traffic demand combinations are considered: i)  $\lambda_1 = \lambda_2 = \lambda_3 = \lambda_4$ ; ii)  $\lambda_1 = \lambda_2 = 2 \times \lambda_3 = 2 \times \lambda_4$ ; iii)  $\lambda_1 = 2 \times \lambda_2 = 4 \times \lambda_3 = 8 \times \lambda_4$ .

### C. Simulation Results

In this section, we present the simulation results obtained from a 100-second simulation run for various traffic demand combinations, as described in Section VI-B. The average aggregate throughput received by the UAV is measured over each one-second simulation time. The results are depicted using the complementary cumulative distribution function (CCDF) to illustrate the distribution of the aggregate throughput across different scenarios.

In Scenario A, shown in Fig. 5, placing the UAV in the optimal position (Position 1 in Fig. 3) leads to significant improvement in aggregate throughput. Specifically, compared to Position 2, the aggregate throughput is enhanced up to 85% for the 90th percentile and up to 80% for the 50th

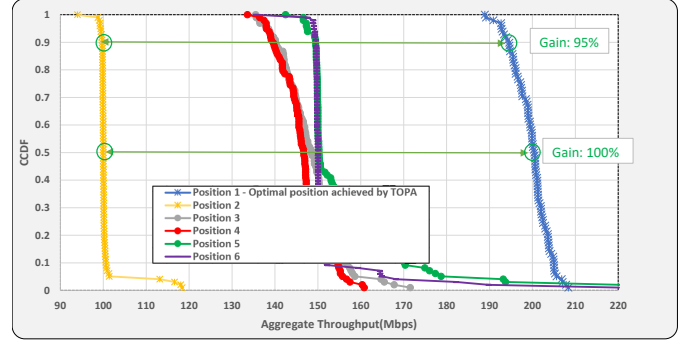


Fig. 6. Scenario B - Aggregate throughput measured on UAV, where  $\lambda_1 = \lambda_2 = \lambda_3 = \lambda_4$ .

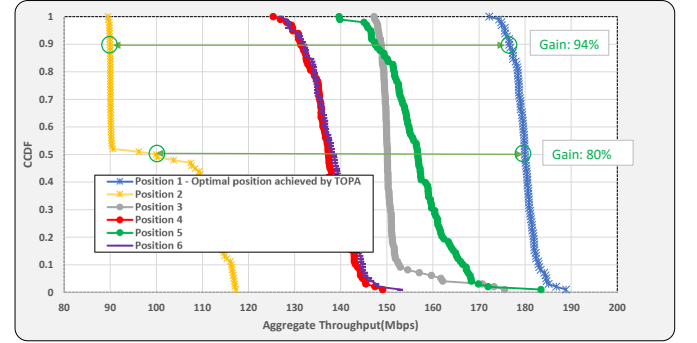


Fig. 7. Scenario B - Aggregate throughput measured on UAV, where  $\lambda_1 = \lambda_2 = 2 \times \lambda_3 = 2 \times \lambda_4$ .

percentile (median). In positions 3 and position 4 the UAV is not in LoS with all UEs. Additionally, considering the varying traffic demand, the aggregate throughput on the UAV differs across these positions.

The performance achieved in scenario B is depicted in Fig. 6, considering all users with the same traffic demand. The aggregate throughput measured on the UAV shows a significant improvement when the UAV is deployed at the optimal position (Position 1). In comparison to Position 2, the aggregate throughput is increased up to 95% for the 90th percentile and 100% for the 50th percentile. The other four positions have similar performance due to the similarity of

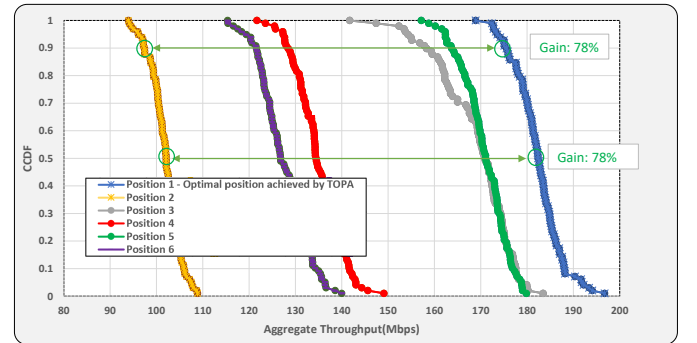


Fig. 8. Scenario B - Aggregate throughput measured on UAV, where  $\lambda_1 = 2 \times \lambda_2 = 4 \times \lambda_3 = 8 \times \lambda_4$ .



their traffic demand, and the fact that each position allows for LoS connectivity with three groups of UEs. In Fig. 7, the traffic demands of  $UE_1$  and  $UE_2$  are twice the other UEs. In that case, the aggregate throughput is enhanced up to 94% for the 90th percentile and 80% for the 50th percentile when compared with Position 2. Finally, for traffic demand  $\lambda_1 = 2 \times \lambda_2 = 4 \times \lambda_3 = 8 \times \lambda_4$ , there is an increase of 78% in the aggregate throughput (illustrated in Fig. 8). As a result, deploying the UAV at the optimal position results in substantial improvements in aggregate throughput, ranging from 80% to 100% across various scenarios. The performance is notably influenced by factors like traffic demand and Line-of-Sight (LoS) connectivity with the users.

## VII. CONCLUSIONS

This work aimed at positioning a UAV in a challenging environment, considering the obstacles in the scenario to establish LoS connections between the UAV and all users. TOPA demonstrates its effectiveness in improving the performance of FNs by optimally positioning the UAV based on traffic demand and ensuring LoS connections. TOPA achieves significant enhancements in aggregate throughput compared to the baseline positions. The results show that the optimal placement of the UAV leads to throughput improvements ranging from 80% to 100%. Overall, the findings highlight the potential of TOPA to optimize aerial networks and provide valuable insights for future research in this domain. For instance, the use of computer vision techniques to detect the position of users and obstacles, as well as the evolution to multi-UAV and multi-obstacle scenarios, can be interesting topics for future works.

## REFERENCES

- [1] H. Yao, R. Qin, and X. Chen, "Unmanned aerial vehicle for remote sensing applications—a review," *Remote Sensing*, vol. 11, no. 12, 2019. [Online]. Available: <https://www.mdpi.com/2072-4292/11/12/1443>
- [2] M. Mozaffari, W. Saad, M. Bennis, Y.-H. Nam, and M. Debbah, "A tutorial on uavs for wireless networks: Applications, challenges, and open problems," *IEEE Communications Surveys & Tutorials*, vol. 21, no. 3, pp. 2334–2360, 2019.
- [3] L. Shi, N. J. H. Marciano, and R. H. Jacobsen, "A survey on multi-unmanned aerial vehicle communications for autonomous inspections," in *2019 22nd Euromicro Conference on Digital System Design (DSD)*, 2019, pp. 580–587.
- [4] I. Bucaille, S. Héthuin, A. Munari, R. Hermenier, T. Rasheed, and S. Allsopp, "Rapidly deployable network for tactical applications: Aerial base station with opportunistic links for unattended and temporary events absolute example," in *MILCOM 2013 - 2013 IEEE Military Communications Conference*, 2013, pp. 1116–1120.
- [5] Q. Wu and R. Zhang, "Common throughput maximization in uav-enabled ofdma systems with delay consideration," *IEEE Transactions on Communications*, vol. 66, no. 12, pp. 6614–6627, 2018.
- [6] E. N. Almeida, A. Coelho, J. Ruela, R. Campos, and M. Ricardo, "Joint traffic-aware uav placement and predictive routing for aerial networks," *Ad Hoc Networks*, vol. 118, p. 102525, 2021. [Online]. Available: <https://www.sciencedirect.com/science/article/pii/S1570870521000779>
- [7] A. Coelho, H. Fontes, R. Campos, and M. Ricardo, "Traffic-aware gateway placement for high-capacity flying networks," in *2021 IEEE 93rd Vehicular Technology Conference (VTC2021-Spring)*, 2021, pp. 1–6.
- [8] A. Coelho, E. N. Almeida, P. Silva, J. Ruela, R. Campos, and M. Ricardo, "Redefine: Centralized routing for high-capacity multi-hop flying networks," in *2018 14th International Conference on Wireless and Mobile Computing, Networking and Communications (WiMob)*, 2018, pp. 75–82.
- [9] A. Coelho, R. Campos, and M. Ricardo, "Proactive queue management for flying networks," in *2020 IEEE 31st Annual International Symposium on Personal, Indoor and Mobile Radio Communications*, 2020, pp. 1–6.
- [10] P. Yi, L. Zhu, L. Zhu, Z. Xiao, Z. Han, and X.-G. Xia, "Joint 3-d positioning and power allocation for uav relay aided by geographic information," *IEEE Transactions on Wireless Communications*, vol. 21, no. 10, pp. 8148–8162, 2022.
- [11] M. Mozaffari, W. Saad, M. Bennis, and M. Debbah, "Efficient deployment of multiple unmanned aerial vehicles for optimal wireless coverage," *IEEE Communications Letters*, vol. 20, no. 8, pp. 1647–1650, 2016.
- [12] J. Lyu, Y. Zeng, R. Zhang, and T. J. Lim, "Placement optimization of uav-mounted mobile base stations," *IEEE Communications Letters*, vol. 21, no. 3, pp. 604–607, 2017.
- [13] D. Marasinghe, N. Rajatheva, and M. Latva-aho, "Lidar aided human blockage prediction for 6g," in *2021 IEEE Globecom Workshops (GC Wkshps)*, 2021, pp. 1–6.
- [14] G. Charan, M. Alrabeiah, and A. Alkhateeb, "Vision-aided dynamic blockage prediction for 6g wireless communication networks," in *2021 IEEE International Conference on Communications Workshops (ICC Workshops)*, 2021, pp. 1–6.
- [15] T. Nishio, Y. Koda, J. Park, M. Bennis, and K. Doppler, "When wireless communications meet computer vision in beyond 5g," *IEEE Communications Standards Magazine*, vol. 5, no. 2, pp. 76–83, 2021.
- [16] Z.-A. Deng, Z. Qu, C. Hou, W. Si, and C. Zhang, "Wifi positioning based on user orientation estimation and smartphone carrying position recognition," *Wireless Communications & Mobile Computing (Online)*, vol. 2018, 2018.
- [17] "Wireless lan professional," Website, accessed: 05 30, 2023. [Online]. Available: <https://wlanprofessionals.com/mcs-table-and-how-to-use-it/>